JOURNAL
OF THE AMERICAN CHEMICAL SOCIETY

VOLUME 96, NUMBER 6 MARCH 20, 1974

An Absolute Measurement of the Rate Constant for Isopropyl Radical Combination[1a]

D. M. Golden,* L. W. Piszkiewicz, M. J. Perona,[1b] and P. C. Beadle[1b]

Contribution from the Department of Thermochemistry and Chemical Kinetics, Stanford Research Institute, Menlo Park, California 94025.
Received October 10, 1973

Abstract: Absolute values of the rate constant for isopropyl radical combination have been determined over the temperature range 683–808°K. The value $\log k_r\ (M^{-1}\ \mathrm{sec}^{-1}) = 9.5 \pm 0.2$ fits all the data, leading to the conclusion that the temperature dependence, if any, is slight. The compatibility of this value with other values determined either directly or from the reverse process *via* thermochemical data depends on the particular model chosen to represent the transition state since the temperatures of the various determinations differ. It has been found that isopropyl radicals react heterogeneously in a first-order manner with fused silica, probably to produce propylene.

Almost all "absolute" values for the rate constants of radical–molecule processes are deduced from measurements relative to radical–radical processes, few of whose rate constants have actually been determined. In those cases where determinations have been made, there is rarely any measure of the dependence on temperature, and there is often a good deal of uncertainty concerning the data.

These facts have been noted recently by Kerr[2] who states, "The importance of the absolute measurements of the rates of radical combinations can hardly be overemphasized." With this thought as our charge, this laboratory has embarked on a program of measuring absolute values for radical–radical processes by several techniques. There have been reports[3] on values obtained at relatively low temperatures mostly by the radical–buffer technique,[3a–e] and this is the first formal report[4] on absolute values as determined by the very low-pressure pyrolysis (VLPP) technique.

Background

In several prior publications[5,6] from this laboratory, we have discussed the use of the VLPP technique to measure rate constants for unimolecular reactions. We have also presented some work showing the usefulness of VLPP for determining absolute rate constants for radical–molecule reactions[7] and for the measurement of the equilibrium constant for the combination of allyl radicals to form hexa-1,5-diene.[8] We have indicated in a review article[6] the basis for measuring absolute values of the rate constants for radical–radical combination, but as this is the first publication of complete results on a radical system, we will discuss the appropriate treatment in some detail.

If a substance RYR that generates the free radicals R *via* pyrolysis to 2R + Y is introduced into a VLPP reactor (which is a stirred-flow reactor with the lifetime for escape of any species, A, given by the Knudsen equation), the history of the radicals can be described in terms of first- and second-order loss processes having the rate constants k_1 and k_2 with appropriate units. Thus, if f represents the fraction of RYR decomposed

(1) (a) This work was supported, in part, under Contract F44620-71-C-0103 with the Air Force Office of Scientific Research, which we gratefully acknowledge; (b) postdoctoral research associate.
(2) J. A. Kerr, "Free Radicals," J. K. Kochi, Ed., Wiley, New York, N. Y., 1973, Chapter 2.
(3) (a) R. Hiatt and S. W. Benson, *J. Amer. Chem. Soc.*, **94**, 25 (1972); (b) R. Hiatt and S. W. Benson, *ibid.*, **94**, 6886 (1972); (c) R. Hiatt and S. W. Benson, *Int. J. Chem. Kinet.*, **4**, 151 (1972); (d) R. Hiatt and S. W. Benson, *ibid.*, **5**, 385 (1973); (e) R. Hiatt and S. W. Benson, *ibid.*, 4, 479 (1972); (f) D. F. McMillen, D. M. Golden, and S. W. Benson, *J. Amer. Chem. Soc.*, **94**, 4403 (1972).
(4) P. C. Beadle, M. J. Perona, and D. M. Golden, Annual Report to AFOSR on Contract F44620-71-C-0103, 1972.
(5) (a) K. D. King, D. M. Golden, G. N. Spokes, and S. W. Benson, *Int. J. Chem. Kinet.*, **3**, 411 (1971); (b) G. N. Spokes and S. W. Benson, *J. Amer. Chem. Soc.*, **89**, 2525 (1967).
(6) D. M. Golden, G. N. Spokes, and S. W. Benson, *Angew. Chem., Int. Ed. Engl.*, **12**, 534 (1973).
(7) N. A. Gac, D. M. Golden, and S. W. Benson, *J. Amer. Chem. Soc.*, **91**, 3091 (1969).
(8) D. M. Golden, N. A. Gac, and S. W. Benson, *J. Amer. Chem. Soc.*, **91**, 2136 (1969).

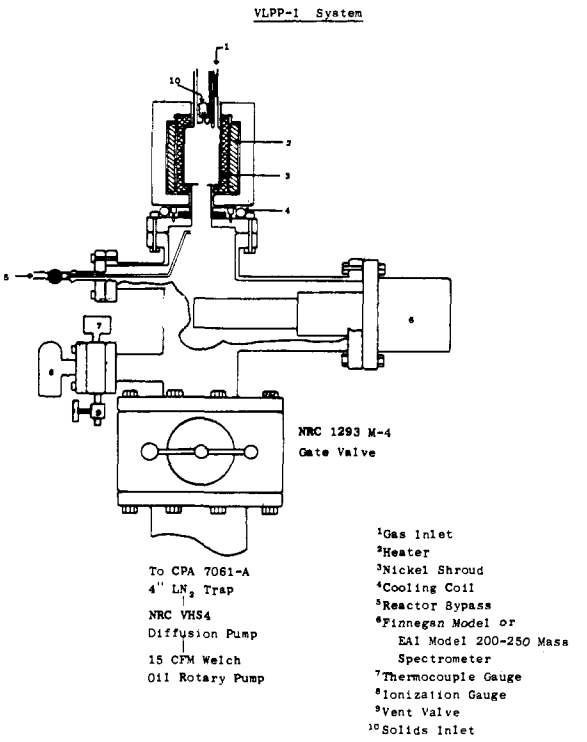

Figure 1. VLPP-I system.

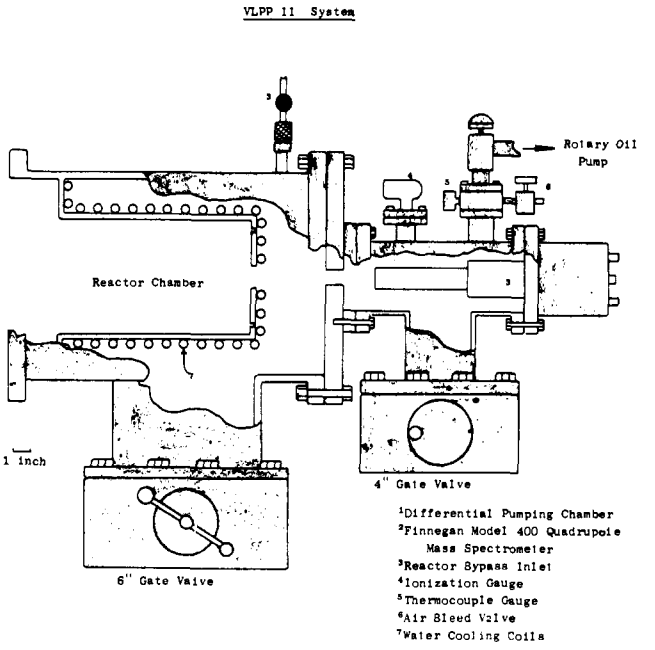

Figure 2. VLPP-II system.

and F_{R_2Y} represents the flow rate of RYR into the reactor, $2fF$ is the initial flux of radicals formed. This must be equal to the flux of radical disappearance by the aforementioned first- and second-order processes

$$2fF_{R_2Y}/V = 2k_2[R]^2 + k_1[R] \quad (1)$$

where [R] is the steady-state concentration of radicals in the reactor. If we denote by the symbol k_r the rate constant for radical combination to form the compound R_2 then the flux of R_2, denoted F_{R_2}, must be given by

$$F_{R_2} = k_r[R]^2V \quad (2)$$

Combining (1) and (2), we get[9]

$$\frac{fF_{R_2Y}}{F_{R_2}} = \frac{k_2}{k_r} + \frac{k_1V^{1/2}}{2k_r^{1/2}F_{R_2}^{1/2}} \quad (3)$$

If, as we might expect, the only first-order loss process were escape, $k_1 = k_{eR}$. If, also, k_2 were the sum of rate constants for combination (k_r) and disproportionation (k_d), we may write

$$\frac{fF_{R_2Y}}{F_{R_2}} = 1 + \frac{k_d}{k_r} + \frac{k_{eR}V^{1/2}}{2k_r^{1/2}F_{R_2}^{1/2}} \quad (4)$$

We see from eq 4 that a plot of the directly measurable quantities fF_{R_2Y}/F_{R_2} *vs.* $F_{R_2}^{-1/2}$ (the Brauman plot) should yield a straight line with slope $k_{eR}V^{1/2}/2k_r^{1/2}$ and intercept $1 + k_d/k_r$, thus leading to absolute values for both k_r and k_d, since k_{eY} is known from the reactor geometry.

In principle, such a procedure can be carried out in a reactor with given aperture size, from a temperature limited at the lower end by the decomposition rate of RYR and at the upper end by decomposition of the radicals to give olefins plus smaller radicals or H atoms, yielding the temperature dependence of both k_d and k_r.

It must be kept in mind that for the smaller radicals, k_r may not be at its high pressure limit and the ratio of k_d/k_r may be indicative of the degree of falloff if compared with known values of $(k_d/k_r)_\infty$.

In this work RYR was azoisopropane (AIP) and R_2 was 2,3-dimethylbutane (DMB).

Experimental Section

Apparatus. Two different VLPP apparatuses, shown in Figures 1 and 2, were used in this work. For convenience we refer to the simpler single pumped system of Figure 1 as VLPP-I and the other as VLPP-II. The double pumping in VLPP-II allows the use of somewhat higher flow rates than in VLPP-I, but we observe no difference in results using either system.

The mass spectrometers in each system are Finnigan 400 residual gas analyzers equipped with preamplifiers (Finnigan Instruments, Sunnyvale, Calif.). The pumps, traps, gate valves, etc., are standard items. Gases are stored in large (5-l.) bulbs and leaked into the reactor *via* a series of capillaries. Flow rates are measured by monitoring the pressure drop in a calibrated volume using pressure transducers (Pace Model 7D, modified for vacuum use).

The triple-aperture reactor used in VLPP-I has been described previously.[5] Two different reactors were used in VLPP-II. Reactor A was a simple, single-aperture reactor with a collision number of $Z = 2203$, and reactor B was a newly designed triple-aperture reactor shown in Figure 3. Important reactor dimensions and computed quantities are shown in Table I.

Although the relationships between reactor dimensions and the lifetime within the reactor have been discussed previously,[5] certain effects of the exit tube were omitted from the discussion, and the key relationships will be reviewed here.

Reactors are cylindrical, and escape apertures are bevelled conical orifices with larger diameters on the outside (mass spectrometer side) than on the inside (reactor side). When computing the lifetime within the reactor, we must take into account the finite thickness of the aperture, and the area of the hole (A_h), computed from the radius on the inside (r_h), must be multiplied by the Clausing factor[5] of the hole (C_h) to yield the effective aperture area (A_{he}).

There must also be a correction to account for the fact that some molecules that have escaped from the reactor will find their way back into the reactor because of reflections from the walls of the exit tube.

If the flux down the exit tube is φ, the flux at the end is $C_t\varphi$, where C_t is the Clausing factor of the tube. Thus $(1 - C_t)\varphi$ is reflected

(9) Since the basic form for this equation was suggested by Professor J. I. Brauman of Stanford University during his sabbatical residence in this laboratory, we have come to call this the "Brauman equation."

Table I. Reactor Parameters

	VLPP–I	VLPP–II A	VLPP–II B
Aperture diameter (cm) = $2r_h$	0.979		0.940
($A_h = \pi r_h^2$)	0.332	0.2	0.367
	0.103		0.160
Clausing factor (aperture) = C_h/C_h'	0.78/0.78		0.937/0.506
Escape direction = C_h	0.95/0.51	0.94/0.24	0.967/0.349
Reentry direction = C_h'	0.93/0.079		0.914/0.227
Clausing factor (exit tube) = C_t	0.58	0.31	0.052
Area of reactor base (cm²) = A_b	5.02	5.1	15.5
Exit tube correction factor = Q	0.922		0.71
$Q = \left[1 - \frac{(1 - C_t)A_{he}'/A_b)}{1 - (1 - C_t)(1 - A_{he}'/A_b)}\right]$	0.994	0.91	0.96
($A_{he}' = A_h C_h'$)	1.00		0.995
Volume (cm³) = V	136.8	30	110.7
k_{eh} (sec^{-1}) = $k_e Q$ = $(3.65 \times 10^3)\frac{A_{he}Q}{V}\left(\frac{T}{M}\right)^{1/2}$	14.4 $(T/M)^{1/2}$		15.2$(T/M)^{1/2}$
	2.18 $(T/M)^{1/2}$	3.3$(T/M)^{1/2}$	3.20$(T/M)^{1/2}$
	0.207 $(T/M)^{1/2}$		0.604$(T/M)^{1/2}$
($A_{he} = A_h C_h$)			
Surface area (cm²) = A_w	152	63	120.6
Collision number = $Z = A_w/(A_{he}Q)$	281		326
	1863	2203	1342
	19,613		6688
Collision frequency (sec^{-1}) = $\omega = Zk_{eh} = \frac{3.65 \times 10^3 A_w}{V}\left(\frac{T}{M}\right)^{1/2}$	$4.06 \times 10^3(T/M)^{1/2}$	$7.7 \times 10^3(T/M)^{1/2}$	$3.98 \times 10^3(T/M)^{1/2}$

back on the first pass, of which $(1 - C_t)\varphi A_{he}'/A_b$ gets back into the reactor, where A_{he}' is the effective area of the aperture in the direction from the exit tube into the reactor and A_b is the area of the upper end of the tube (the base *plate* of the reactor). This leaves $(1 - C_t)\varphi(1 - A_{he}'/A_b) = \varphi'$ to have a second try at getting out of the tube, but only $C_t\varphi'$ makes it out with $(1 - C_t)\varphi'$ being reflected back and $(1 - C_t)\varphi'(A_{he}'/A_b)$ going back into the reactor and $(1 - C_t)\varphi'(1 - (A_{he}'/A_b))$ trying to make it out the third time, and so on.

Thus, the net flux out of the reactor is

$$F = \varphi - (1 - C_t)\varphi\frac{A_{he}'}{A_b} - (1 - C_t)\varphi'\frac{A_{he}'}{A_b} + \dots$$

$$= \varphi\left[1 - (1 - C_t)\frac{A_{he}'}{A_b} - (1 - C_t)^2\frac{A_{he}'}{A_b} \times \left(1 - \frac{A_{he}'}{A_b}\right) + \dots\right]$$

$$= \varphi\left[1 - (1 - C_t)\frac{A_{he}'}{A_b}\left\{1 + (1 - C_t) \times \left(1 - \frac{A_{he}'}{A_b}\right)\right\} + \dots\right]$$

$$= \varphi\left[1 - \frac{(1 - C_t)\frac{A_{he}'}{A_b}}{1 - (1 - C_t)\left(1 - \frac{A_{he}'}{A_b}\right)}\right] \quad (5)$$

Since $\varphi = k_e[S]$, where k_e is the escape constant for the aperture, $k_e = 0.25\bar{C}A_{he}/V$, and [S] is the number of molecules of substance S in steady state in the reactor

$$F = k_e[S]\left[1 - \frac{(1 - C_t)A_{he}'/A_b}{1 - (1 - C_t)(1 - (A_{he}'/A_b))}\right] \equiv k_{eh}[S] \equiv k_e Q[S] \quad (6)$$

The reactors, all fashioned from fused silica, are encased in nickel blocks, which are heated by ceramic heaters, the temperature being monitored by several thermocouples.

Procedure. The experiments were performed in a straightforward manner that may best be described in terms of the numbered steps below.

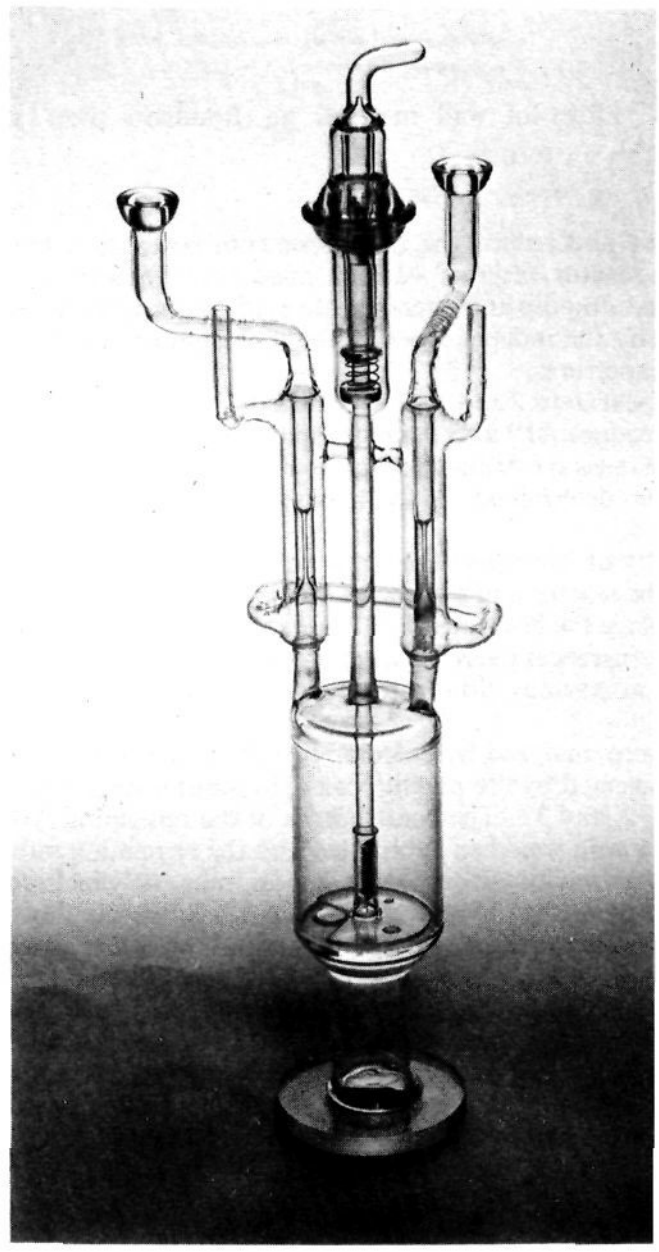

Figure 3. Triple aperture reactor (VLPP-II(B)).

1. Set the temperature of the reactor–oven system to a desired point.
2. Introduce DMB into the mass spectrometer *via* the bypass line, which bypasses the reactor, and record the mass spectrum.
3. Without changing flow rate, switch the flow of DMB through

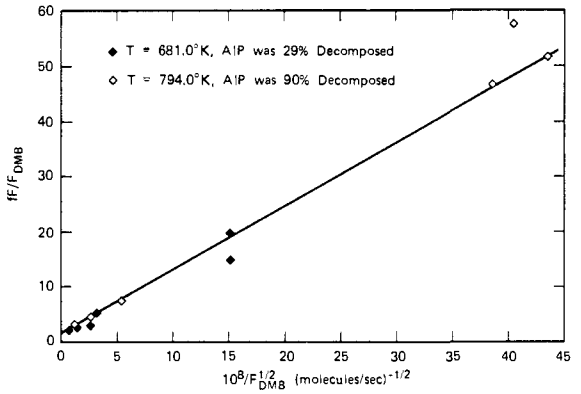

Figure 4. Brauman plot for isopropyl radicals (VLPP-II(A)).

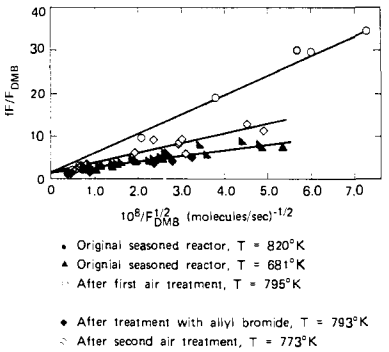

Figure 5. Effect of wall material on Brauman plot. Reactor VLPP-II(A).

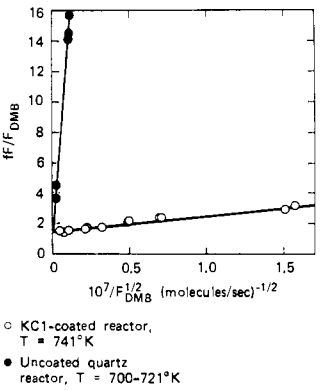

Figure 6. Effect of wall material on Brauman plot. Reactor VLPP-I, $Z = 19{,}613$.

the reactor and record the mass spectrum so as to calibrate the bypass-to-reactor ratio of various mass peak intensities. (DMB does not decompose at the temperatures of these experiments.)

4. Verify the independence of the spectrum to aperture size by changing apertures.

5. Repeat steps 2 and 4 for several different flow rates.

6. Introduce AIP into the mass spectrometer *via* the bypass and record the mass spectrum so that the peak heights in undecomposed AIP can be determined *via* the bypass to reactor ratio determined in steps 2–5.

7. Without changing the flow rate, switch the flow of AIP through the reactor and record the mass spectrum for each aperture.

8. Change the flow rate of AIP and repeat steps 6 and 7.

In some instances the mass spectra of propane and propylene were recorded at various flow rates so that mass balances could be checked.

Data were analyzed by calculating f from the disappearance of AIP as indicated by the parent peak (114 amu) using the data from steps 6, 7, 2, and 3. The contribution of the remaining AIP to the peak of 86 amu was then subtracted and the remaining intensity at 86 amu was attributed to DMB, the amount of which could be computed from the calibrations of step 3. Since the flow rate of AIP, F, was always measured, the data could be plotted according to eq 3.

Propane and propylene sensitivities could also be obtained, so that the amounts of these substances could also be measured. The propylene was measured from the value of the peak at 42 amu and the propane from both the 44- and 29-amu peaks. (Contributions to 42 and 44 amu from C-13 isotopes were subtracted.)

Results

Verification of the Brauman Equation. The earliest tests of eq 3 were carried out in VLPP-II, reactor A. Figure 4 is an example of a "Brauman plot." The linearity is apparent and the value of the intercept is reasonable (*i.e.*, a value greater than unity by an amount that could be a reasonable value of k_d/k_r).

Data of this type can yield k_r from a value for the slope if, in fact, the linearity of Figure 4 means that eq 4 is correct. Actually, eq 3 predicts linearity of the type observed without specifying either the homogeneity of the processes represented by k_1 and k_2 or their nature. That is, there might be other second-order radical processes besides combination and disproportionation, and any of these second-order processes, including combination and disproportionation, could be heterogeneous. Further, there might be other first-order processes besides effusion out of the reactor and these might be heterogeneous as well.

Surface Effects. Figure 5 demonstrates that k_1 contains a heterogeneous component and might better be written as $k_1 = k_{eR} + k_x$, where k_x is some unknown first-order radical loss process. The passage of air through the reactor for several days at 900° before an experiment resulted in an increase in slope by a factor of 4 relative to the original "seasoned" reactor. The slope could be returned to its original value by pyrolyzing allyl bromide in the reactor. Such a treatment resulted in a carbon coating on the reactor wall. A second treatment with air, following the allyl bromide treatment, again raised the slope, but not as much as the first treatment. It appears that treating the reactor with air increased k_x. No changes in product identity were observed as a result of the air treatment. Note that in Figure 5 the intercept is independent of the wall pretreatment.

It was found that coating the reactor wall with KCl greatly reduced the slope of the recombination plot and, presumably, k_x. This effect is shown in Figure 6, where the results shown are from the triple-aperture reactor of VLPP-I, using the smallest aperture.

The invariance of the Brauman plot intercepts to the nature of the surface suggests that the constant k_2 is homogeneous, consisting of k_d and k_r. There remains the possibility that both k_d and k_r are affected in exactly the same manner by the surface. This was shown not to be so, as described below.

Low-Electron Energy Experiments. A series of experiments was carried out in which the electron energy in the mass spectrometer ionizer was reduced from the usual value of 70 to 13 V. The purpose of these experiments was to verify that the formation of DMB was due solely to a process that is homogeneous and second order in radical concentration. Under these experimental conditions, the i-C_3H_7 radical was the main contributor to the m/e 43 peak. Subtraction of the contributions from AIP, DMB, and PrH yielded

Table II. Pyrolysis of AIP at 723°K

F_{AIP}[a]	F_{DMB}[a]	f	fF/F_{DMB}	$F_{DMB}^{-1/2}$[b]	Z	Date
6.10	0.501	0.482	5.87	4.46	1342	2-21-73
17.4	2.36	0.540	3.98	2.06	1342	
3.08	0.174	0.509	9.00	7.58	1342	
8.56	0.907	0.505	4.76	3.32	1342	
26.3	4.11	0.530	3.39	1.56	1342	
4.51	0.363	0.519	6.45	5.25	1342	
39.5	1.06	0.264	9.80	3.08	326	
11.8	0.179	0.241	15.9	7.47	326	
6.71	0.0625	0.228	24.5	12.7	326	2-23-73
18.5	0.360	0.242	12.4	5.27	326	
58.0	2.06	0.250	7.05	2.20	326	
6.31	0.636	0.519	5.20	3.98	1342	
18.7	2.34	0.543	4.34	2.07	1342	
18.3	6.15	0.851	2.53	1.28	6688	
6.05	1.40	0.833	3.60	2.68	6688	
56.2	22.1	0.903	2.30	0.67	6688	
2.58	0.634	0.831	3.38	3.97	6688	
8.09	2.40	0.853	2.88	2.04	6688	
1.05	0.192	0.825	4.30	7.22	6688	
10.1	0.168	0.255	15.3	7.71	326	
29.1	11.3	0.909	2.34	0.94	6688	3-12-73
29.1	6.20	0.632	2.96	1.27	1342	
29.1	0.768	0.270	10.2	3.61	326	
3.34	0.742	0.870	3.91	3.67	6688	
3.34	0.260	0.512	6.57	6.20	1342	
8.69	2.94	0.872	2.58	1.85	6688	
8.69	1.33	0.555	3.62	2.74	1342	
8.69	1.12	0.288	22.3	9.45	326	
26.6	11.8	0.901	2.03	0.92	6688	
26.6	6.60	0.606	2.45	1.23	1342	
26.6	0.787	0.279	9.43	3.57	326	
10.8	0.173	0.280	17.5	7.63	326	
10.8	3.58	0.880	2.65	1.67	6688	
4.55	0.500	0.579	5.27	4.47	1342	
4.55	0.0352	0.285	36.8	16.8	326	
4.55	1.40	0.872	2.83	2.68	6688	
22.8	4.54	0.473	2.38	1.48	1342	3-20-73
22.8	0.515	0.210	9.30	4.41	326	
22.8	9.07	0.890	2.24	1.05	6688	
20.9	3.90	0.617	3.31	1.60	1342	3-21-73
20.9	0.415	0.182	9.17	4.91	326	
20.9	7.60	0.895	2.46	1.15	6688	
59.8	24.5	0.919	2.24	0.64	6688	
59.8	15.0	0.611	2.44	0.82	1342	
59.8	2.30	0.228	5.93	2.09	326	
6.38	2.30	0.846	2.35	2.09	6688	
6.38	0.850	0.593	4.45	3.43	1342	
13.8	5.36	0.870	2.24	1.37	6688	
13.8	2.30	0.497	2.98	2.09	1342	
13.8	0.225	0.205	12.6	6.67	326	
40.4	16.5	0.902	2.21	0.78	6688	
40.4	8.70	0.544	2.53	1.07	1342	
40.4	1.20	0.246	8.28	2.89	326	
4.45	1.12	0.848	3.37	2.99	6688	
4.45	0.465	0.528	5.05	4.64	1342	
4.45	0.020	0.203	45.2	22.4	326	

[a] All fluxes are in units of molecules/sec and have been multiplied by 10^{-15}. [b] Units are (sec/molecule)$^{1/2}$ and values have been multiplied by 10^{8}.

I_{43}^{Pr}, the mass peak intensity due to the i-C_3H_7 radical. A second-order dependence of DMB formation on radical concentration leads to the following equations

$$k_{eDMB}[DMB] = k_r[Pr]^2 \quad (7)$$

$$I_{43}^{Pr} = \alpha_{Pr}F_{Pr} = \alpha_{Pr}k_{ePr}[Pr]V \quad (8)$$

$$I_{86}^{DMB} = \alpha_{DMB}F_{DMB} = \alpha_{DMB}k_{eDMB}[DMB]V \quad (9)$$

where Pr symbolizes the isopropyl radical, I_x^M is the intensity of the mass peak arising from species M and having $m/e = x$, α_M is a calibration factor, and F_M is the flux of M out of the reactor. A combination of eq 7–9 yields

$$\frac{I_{86}^{DMB}}{I_{43}^{Pr}} = \left(\frac{k_r\alpha_{DMB}}{\alpha_{Pr}^2 k_{ePr}^2 V}\right)(I_{43}^{Pr}) \quad (10)$$

According to eq 10, if DMB arises only from second-order radical recombination, a plot of the left-hand side of eq 10 *vs.* I_{Pr} should yield a straight line with an intercept of zero and a slope that is independent of pretreatment of the reactor wall. A positive intercept would be an indication of a first-order source of DMB. Such a plot is shown in Figure 7, and it supports the assumption that DMB production is second order in radicals and is homogeneous.

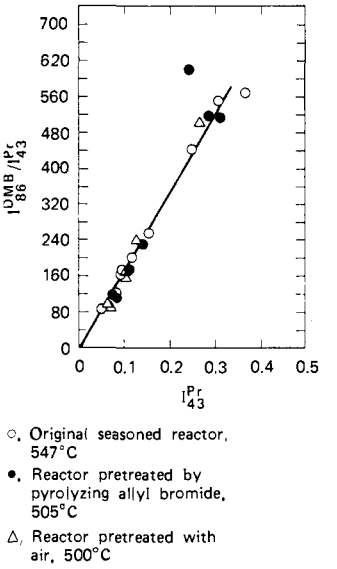

Figure 7. The isopropyl radical low-electron energy data plotted according to eq 10. VLPP-II(A).

The low-electron energy experiments also served to check our analytical techniques. Brauman plots obtained in these experiments were in good agreement with those obtained at 70 V.

Triple-Aperture Reactor. If the previous experiments may be used to conclude that $k_2 = k_d + k_r$ and that $k_1 = k_{eR} + k_x$, eq 4 may be written

$$\frac{fF_{AIP}}{F_{DMB}} = 1 + \frac{k_d}{k_r} + \frac{(k_{ePr} + k_x)V^{1/2}}{2k_r^{1/2}F_{DMB}^{1/2}} \quad (11)$$

Thus, Brauman plots, using any two apertures of a multiaperture VLPP reactor and all other conditions remaining constant, will yield two lines with the same intercept and with different slopes (providing that k_x is not so much greater than k_{ePr} for either aperture that it becomes the only effective loss process) from which k_x and k_r may be computed. Results in the triple-aperture reactor of VLPP-I did, indeed, yield three separate straight lines; however, their slopes are relatively close to each other and are consistent with a value of k_x of about 60 sec^{-1}. Since the values of k_{ePr}/k_x for the three apertures are of the order of 1, 0.1, and 0.01, it is difficult to get accurate information from the slopes of these lines. This led us to seek a way to reduce the value of k_x. Noting that carbonaceous material and KCl both reduced the value of k_x, we chose to coat the reactor VLPP-II(B) with a "gold" coating,[10] using the

(10) Following a suggestion of Mme. Janine Fournier, C.N.R.S., Paris, France.

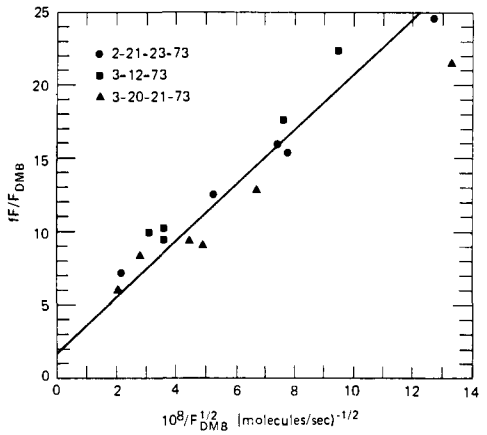

Figure 8. Brauman plots for isopropyl radicals at 723°K; Z = 326 for reactor VLPP-II(B), gold coated.

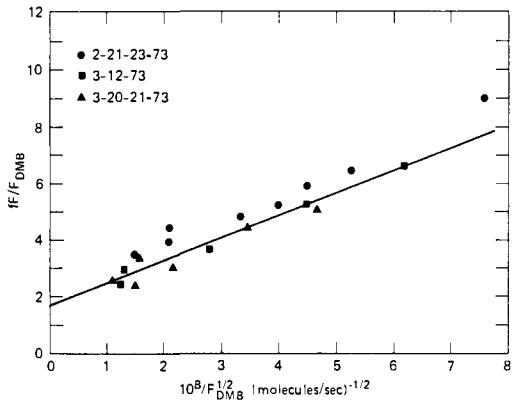

Figure 9. Brauman plots for isopropyl radicals at 723°K; Z = 1342 for reactor VLPP-II(B), gold coated.

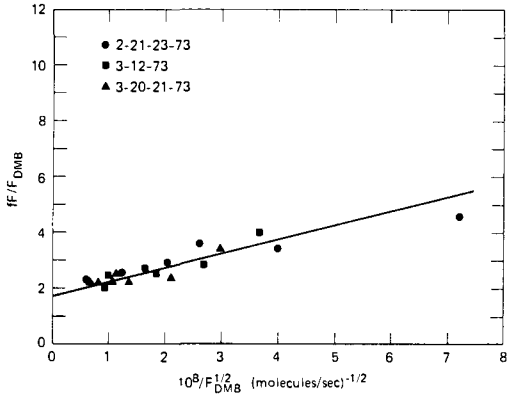

Figure 10. Brauman plots for isopropyl radicals at 723°K; Z = 6688 for reactor VLPP, gold coated. (The line was computed based on Figures 8 and 9.)

commercial product "Liquid Bright Gold" (produced by the Hanovia Division of Englehard Industries). This coating, accomplished by two applications of the liquid substance, is surely not a complete covering, and we were not surprised that k_x did not become zero. However, as can be seen from the following results, k_x was reduced sufficiently to get reportable results. We are testing other coatings.

Data taken at 723°K on several occasions over a period of a month, during which the temperature was changed several times, are shown in chronological

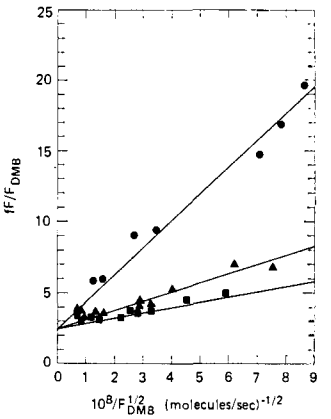

Figure 11. Brauman plot for isopropyl radicals at 768°K in reactor VLPP-II(B), gold coated: (●) Z = 326, (▲) Z = 1342, (■) Z = 6688. (The lower line is computed from the other two lines.)

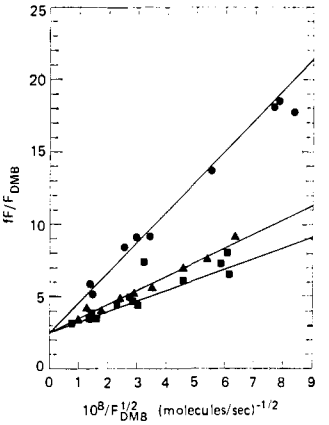

Figure 12. Brauman plot for isopropyl radicals at 808°K in reactor VLPP-II(B), gold coated: (●) Z = 326, (▲) Z = 1342, (■) Z = 6688. (The lower line is computed from the other two lines.)

order in Table II and are plotted in Figures 8–10. The data show some scatter, and perhaps regular trends with time may be discerned, but the overriding features of the Brauman plots are their linearity and their internal consistency. The line shown for Z = 6688 was obtained from solving for k_x and k_r from the slopes in Z = 326 and 1342. The value of the intercept is 1.75, which can be seen to be somewhat arbitrary in the sense that a value of 2.0 would have done no violence to the data and would not change the values for k_r and k_x significantly.

Data of this type were taken at 768 (Figure 11) and 808°K (Figure 12). Data were also taken at 683°K, but the fraction of azo compound decomposed is so low using Z = 326 that only Z = 1342 and 6688 may be used, and the data are considerably less precise than at the higher temperatures.

The values of k_x, k_r, and k_d/k_r are shown in Table III. The values of k_r are substantially the same over the

Table III. Summary of Results

T, °K	k_x, sec^{-1}	$10^{-9}k_r$, M^{-1} sec^{-1}	k_d/k_r
683	5.30	2.46	1.00
723	18.5	3.05	0.75
768	12.9	2.75	1.4
808	31.5	3.56	1.5

Table IV. Mass Balance Data

F_{AIP}[a]	F_{AIP}[a]	F_{DMB}[a]	F_{PrH}[a]	$F_{C_3H_6}$[a]	F_{Pr}[a,b]	M_1[c]	M_2[d]	Z	T, °K
65.2	1.56	26.0	24.5	54.5	2.03	1.04	1.02	6688	768
65.2	10.8	20.8	20.5	50.1	9.62	1.10	1.03	1342	768
65.2	36.8	7.86	8.95	19.7	28.1	1.12	0.905	326	768
6.67	0.260	2.10	2.77	6.33	0.577	1.08	1.04	6688	768
6.67	1.12	1.32	2.02	5.76	7.42	1.13	0.949	1342	768
6.67	3.36	0.262	0.860	3.95	5.13	1.29	0.905	326	768
59.8	4.84	24.5	18.2	34.8	1.81	0.948	0.933	6688	723
59.8	23.3	15.0	12.3	37.3	7.51	1.12	1.06	1342	723
59.8	46.2	2.30	4.26	9.07	14.0	1.04	0.921	326	723

[a] 10^{-15} molecule sec^{-1}. [b] Computed according to eq 12. [c] $[F_{AIP} + F_{DMB} + {}^1/_2F_{PrH} + {}^1/_2F_{C_3H_6} + {}^1/_2F_{Pr}]/F_{AIP}$. [d] $M_1 - {}^1/_2F_{Pr}/F_{AIP}$.

temperature range investigated and may be compatible with a value of the activation energy for combination of 0–3 kcal/mol over this temperature range.

The values of k_d/k_r obtained by subtracting 1.00 from the values of the intercepts are probably valid only to within ±0.5. For isopropyl radicals at room temperature, $k_d/k_{r\infty} = 0.69$. The only measurement of the temperature dependence of this ratio in the gas phase is that of Klein,[11] *et al.*, who obtained $k_d/k_{r\infty} = (0.4 \pm 0.1)\exp(260 \pm 25)/RT$ over the temperature range 77 to 380°K. This result was based on an Arrhenius plot that included data points obtained in both the gas phase and the liquid phase. From the results of Klein, *et al.*, we find that at 750°K, $k_d/k_{r\infty} = 0.67$. Because k_r may be in the falloff pressure region, we expected that at 740°K $(k_d/k_r)_{obsd} \geq 0.67$, and this was observed.

The values of k_x shown in Table III vary with temperature in a way that is compatible with an activation energy in the range of 8–16 kcal/mol.

Mass Balance. It would seem plausible that, whatever the detailed nature of the process described by the rate constant k_x, the surface reaction should produce propane or propylene or both. Thus, a measure of the flux of propane and propylene could lead to a check of the carbon mass balance if the flux of isopropyl radicals could also be taken into account.

The flux of isopropyl radicals, F_{Pr}, can be computed from the rate constant according to

$$F_{Pr} = k_{ePr}\sqrt{\frac{F_{DMB}V}{k_r}} \qquad (12)$$

and a mass balance can be attempted. Unfortunately, the radicals effusing from the reactor may indeed do so with a flux, F_{Pr}, but they may (and almost surely do) react with surfaces on the way to the mass spectrometer yielding propane or propylene or both. The results of a detailed analysis of experiments at two flow rates at 768°K and one flow rate at 723°K are shown in Table IV. There are some striking features. First, the propylene flux is always greater than the propane flux by about a factor of 2. This may suggest that the process denoted by k_x is a heterogeneous reaction producing propylene. Perhaps

$$S + \dot{\wedge} \xrightarrow{x} \wedge\!\!\wedge + S\text{–}H \qquad (13)$$

where S is a surface site.

Second, the mass balance M_1, which is defined in a way that will overcount any radical species that are subsequently detected in the form of propane or propylene after escaping from the Knudsen cell, is generally higher than the theoretical maximum value of unity. The quantity M_2, which is defined in a way that will undercount those radical species that are not detected as propane or propylene subsequent to escape from the reactor, is generally lower than the theoretical value of unity, indicating that some radicals show up as C_3H_8 and C_3H_6 and others do not.

The quantities M_1 and M_2 are both close enough to unity that the carbon mass balance is reasonably well established. We have tried to understand the mass balance data more quantitatively, but the present data are not accurate enough for more quantitative conclusions to be drawn. A referee has pointed out that a plot of F_{PrH}/F_{DMB} *vs.* F_{Pr}/F_{DMB} yields intercepts which should reflect the value of k_d/k_r under conditions of no PrH formation from Pr radicals escaping the reactor. These numbers are 0.72 at 723 K°, to be compared with 0.75 from Table III, and 0.92 at 768°K, to be compared with 1.4. The latter change will affect the Brauman plot slopes very little, but the high-flow points (the ones near the intercept) will deviate somewhat from the lines drawn through new intercepts.

Discussion

The values of k_r from Table III allow us to conclude that in the temperature range 700–800°K, log k_r (M^{-1} sec^{-1}) = 9.5 ± 0.2. We also conclude that this represents the high-pressure value, or very close to it, based on the values of k_d/k_r from the intercept and on the fact that values obtained with the small aperture are in agreement with those obtained from the two bigger apertures even though, at the flow rates employed, the collision frequency in the small aperture reactor was as high as ten times that in the large aperture reactor because of gas–gas collisions. Certainly the values of k_r are greater than ${}^1/_2k_{r\infty}$.

The number of other gas-phase values of k_r that have been reported are limited. A recent study in this laboratory[3c] using the "radical buffer" technique led to a value of log k_r (M^{-1} sec^{-1}) = 8.6 ± 1.1 at 415°K. This compares with an earlier value[12] of log k_r (M^{-1} sec^{-1}) = 10.8, from rotating sector experiments over the range 354–442°K, which certainly seems too high.

The rate constant for combination of isopropyl radicals measured in this work allows us to predict the rate constant for the reverse reaction, the C–C bond homolysis in 2,3-dimethylbutane in the temperature range 700–800°K. We may then compare this predicted value with measured values of the homolysis rate constant.

(11) R. Klein, M. D. Scheer, and R. Kelley, *J. Phys. Chem.*, **68**, 598 (1964).

(12) E. L. Metcalfe and A. F. Trotman-Dickenson, *J. Chem. Soc.*, 4620 (1962).

Table V. Thermochemical Parameters[a] for the Reaction 2,3-Dimethylbutane (A) $\underset{2}{\overset{1}{\rightleftarrows}}$ 2(Isopropyl Radicals (B))[e]

		$S°_{298}$	87.4		68.8		67.0		$\therefore \Delta H°_{1,2(298°K)}$		78.9		78.9					
		$\Delta H_f°_{298}$	−42.5		18.2 (v = 0)		18.2 (v = 2[b])		$\Delta S°_{1,2(298°K)}$		50.2 (v = 0)		46.6 (v = 2[b])					
		$C_p°(T)$								Correction to $\Delta S°_{1,2}$,								
		B						$\Delta H_1°$, kcal		cal deg^{-1} mol^{-1}		$\Delta S°_{1,2}$, cal		$\Delta S°_{1,2} - 4.576$	Log A_1 (sec^{-1})/		$\Delta E°_{1,2}$, kcal	
				$\Delta C_p°(T)$		$\Delta C_p°(T_m)$		mol^{-1}	2.303 log	deg^{-1} mol^{-1}		log ($eR'T$),[d]		A_2 (l. mol^{-1} sec^{-1})		mol^{-1}	
T, °K	A	v = 0	v = 2	v = 0	v = 2	v = 0	v = 2	v = 0	v = 2	T_2/T_1	v = 0	v = 2	v = 0	v = 2	v = 0	v = 2	v = 0	v = 2
1	0	0	0	0	0	−0.8	0.0	79.5	78.8	−4.61	3.59	0	56.3	45.9	59.3	48.9	12.9	10.7	79.5	78.8
100	11.8	5.1	5.9	−1.6	0.0	−2.1	0.4	79.4	78.8	−0.69	1.45	−0.28	52.7	45.9	46.5	39.7	10.2	8.7	79.2	78.6
200	23.0	10.2	11.9	−2.6	0.8	−2.9	1.0	79.2	78.8	−0.41	1.19	−0.41	51.4	46.2	43.8	38.6	9.6	8.4	78.8	78.4
300	33.8	15.3	17.5	−3.2	1.2			78.9	78.9				50.2	46.6	41.8	38.2	9.2	8.4	78.3	78.3
400	43.3	19.6	21.4	−4.1	−0.5	−3.7	0.4	78.5	78.9	0.30	−1.05	0.10	49.1	46.7	40.2	37.8	8.8	8.3	77.7	78.1
500	51.9	23.6	24.8	−4.7	−2.1	−4.4	−1.3	78.1	78.8	0.21	−0.94	−0.30	48.2	46.4	38.8	37.0	8.5	8.1	77.1	77.8
600	59.2	27.1	28.2	−5.0	−2.8	−4.9	−2.5	77.5	78.6	0.18	−0.88	−0.46	47.3	45.9	37.6	36.2	8.2	7.9	76.3	77.6
700	65.4	30.2	30.8	−5.0	−3.8	−5.0	−3.3	77.0	78.3	0.15	−0.75	−0.50	46.5	45.4	36.5	35.4	8.0	7.7	75.6	76.9
800	70.7	32.9	33.5	−4.9	−3.7	−4.9	−3.8	76.5	77.9	0.13	−0.64	−0.49	45.9	44.9	35.6	34.6	7.8	7.6	74.9	76.3
900	75.2	35.3	35.8	−4.6	−3.6	−4.8	−3.7	76.0	77.5	0.11	−0.53	−0.41	45.4	44.5	34.9	34.0	7.6	7.6	74.2	75.7
1000	79.1	37.4	37.8	−4.3	−3.5	−4.4	−3.6	75.6	77.1	0.10	−0.44	−0.36	45.0	44.1	34.2	33.3	7.5	7.3	73.6	75.1
1100	82.3	39.2	39.7	−3.9	−2.9	−4.1	−3.2	75.2	76.8	0.09	−0.37	−0.29	44.6	43.8	33.7	32.9	7.4	7.2	73.0	74.6
1200	85.2	40.7	41.1	−3.8	−3.0	−3.8	−3.0	74.8	76.5	0.09	−0.34	−0.27	44.3	43.5	33.2	32.4	7.3	7.1	72.4	74.1
1300	87.8	42.1	42.3	−3.6	−3.2	−3.7	−3.1	74.4	76.2	0.08	−0.30	−0.25	44.0	43.2	32.7	31.9	7.2	7.0	71.8	73.6
1400	90.2	43.3	43.6	−3.6	−3.0	−3.6	−3.1	74.0	75.9	0.08	−0.29	−0.25	43.7	43.0	32.3	31.6	7.1	6.9	71.2	73.1
1500	92.6	44.3	44.7	−4.0	−3.2	−3.8	−3.1	73.6	75.6	0.08	−0.30	−0.25	43.4	42.7	31.8	31.1	7.0	6.8	70.6	72.6

[a] H. E. O'Neal and S. W. Benson, "Free Radicals," Vol. II, J. K. Kochi, Ed., Wiley, New York, N. Y., 1973, Chapter 17. [b] Barrier to methyl rotation in the radical. [c] For small temperature ranges: $\Delta H°_{T_2} = \Delta H°_{T_1} + \Delta C_p(T_m)(T_2 - T_1) = \Delta E°_{T_2} + RT_2$; $\Delta S°_{T_2} = \Delta S°_{T_1} + \Delta C_p(T_m)2.303 \log (T_2/T_1)$; $\log [A_1 (\text{sec}^{-1})/A_2 (M^{-1} \text{sec}^{-1})] = [\Delta S°_{1,2} - 4.576 \log (eR'T)]/4.576$. [d] Units of cal deg^{-1} mol^{-1}.

Unfortunately, there are no data for the latter values at these temperatures. Therefore, this comparison requires some statement concerning the heat capacity of the transition state, which in turn demands a transition-state model. Thus, we may extrapolate the values of Tsang[13] from 1100°K using his reported Arrhenius parameters (the assumption that Arrhenius parameters are temperature independent is identical with the assumption that the mean heat capacity of activation, $\overline{\Delta C^{\pm}}$, is equal to R, the gas constant), or we may use the transition-state parameters which we find explain the VLPP results on 2,3-dimethylbutane.

Table V shows values of log [A_1 (sec^{-1})/A_2 (M^{-1} sec^{-1})] and $\Delta E°_{1,2}$ for intervals of 100° from 0–1500°K. From the values at 700°K and the assumption that log k_r = log A_2, we see that log k_f (sec^{-1}) = 17.2 − 76.9/θ at 700°K, if we assume that the barrier to methyl rotation in isopropyl radicals is 2 kcal/mol. This compares with Tsang's value[13] of log k_f (sec^{-1}) = 16.4 − 76.5/θ, which is a factor of 5 lower. (Tsang's value corresponds to log k_r (M^{-1} sec^{-1}) = 8.8 at 1100°K.)

We have also done VLPP pyrolysis studies on DMB[14] in an attempt to measure the reaction of interest in both directions. Unfortunately, the temperatures at which we could collect data on the decomposition of DMB were 950–1250°K, so that once again a transition-state model would be required. Of course, such a model must be constructed in order to obtain high-pressure parameters from the VLPP work in any case, although it is well known that only the value of the Arrhenius parameters determines the degree of "falloff," not the details of the model. We find that, if we assign Tsang's parameters to the VLPP results for DMB cracking, the predicted [RRK(M)] rate constants lie somewhat below the data, whereas if we assign the parameters computed from the radical combination rate constant reported here, the computed rate constants are equally too high. The result is that if we fix the A factors and adjust the activation energy to fit the VLPP data, either of the following Arrhenius expressions fit the data over the entire VLPP temperature range

$$\log k_f^{I} (\text{sec}^{-1}) = 16.4 - 74.6/\theta$$

$$\log k_f^{II} (\text{sec}^{-1}) = 17.2 - 78/\theta$$

The value of k_f^{I} is certainly close to Tsang's value (a factor of ~2 lower at 1100°K); the value of k_f^{II} yields a value of log k_r (M^{-1} sec^{-1}) = 9.3, which is the same as the value measured here for 700–800°K, within error limits, where k_f^{I} yields 8.9 for the same value.

It is very difficult to draw any conclusions about the relative merits of the values obtained from different experimental techniques. It is important to understand the consequences of various transition-state models on values of the combination rate constant at various temperatures.

To summarize, there exist three values (barring the rotating sector experiment) for k_r that do not depend on the transition-state model (see Table VI). On first blush, the values for 2 and 3 appear to be in good agreement; unfortunately, this may not be so. The usually accepted transition-state model involves the assignment of the central C–C stretch in DMB as

(13) W. Tsang, *J. Chem. Phys.*, 43, 352 (1965).
(14) Z. B. Alfassi, P. C. Beadle, and D. M. Golden, *Int. J. Chem. Kinet.*, submitted for publication.

Table VI

	log k_r, M^{-1} sec^{-1}	T, °K	Technique
1	9.5 ± 0.2	700–800	VLPP, this work
2	8.6 ± 1.1	415	Radical buffer (includes thermochemistry)
3	8.8 ± ?	~1100	Single-pulse shock tube, reverse reaction, plus thermochemistry

the reaction coordinate, the lengthening of that bond by ~1 Å with the internal rotation about it being rendered free, and the weakening of the four bending modes, which are destined to become free rotations of the isopropyl radicals, to a frequency value anywhere from a fifth to a tenth of the values in DMB. If one uses this sort of model, one cannot fit the data, such as to predict essentially no temperature dependence for recombination of isopropyl radicals over the 700° temperature range represented by values 2 and 3 above. In fact, if one assigns the transition-state parameters, such that the value for k_f agrees with Tsang's parameters at 1100°K (leading to value 3 above), one predicts a value of log k_r (M^{-1} sec^{-1}) = 9.2 at 400°K. On the other hand, an assignment of transition-state parameters, such that the value of k_f agrees with the value of k_f at 700°K derivable from this work (value 1 above), leads to a value of log k_r (M^{-1} sec^{-1}) = 8.6 at 400°K. It should also be pointed out that since ΔE_{100} = 78.1 kcal/mol, both results have to be accommodated with a negative value of activation energy for the radical combination, a phenomenon whose origins are extremely unclear. More than likely the transition-state model is not correct, and the assignment of the low-frequency bending modes is open to question. An alternative model in which these motions are treated as restricted external rotations having less heat capacity than vibrational modes is considered elsewhere.[15]

In conclusion, the value for k_r measured here is $10^{9.5\pm0.2}$ M^{-1} sec^{-1}, which is in seeming disagreement with the value derivable from Tsang's[13] single-pulse shock tube pyrolysis of DMB and with the radical buffer[3c] value by a factor of ~5. Compatibility with either value depends on transition-state models, since the temperatures differ.

It should also be noted in conclusion that the single biggest difficulty in this work, namely the propensity for alkyl radials to react in a first-order manner at the walls of the reactor, gives us cause to be concerned for some of the extant values of radical reaction rate constants.

Acknowledgments. Discussions with S. W. Benson were, as always, incisive and inspiring. J. I. Brauman's contributions, while specifically mentioned in the text, deserve special acknowledgment for their spiritual quality as well.

(15) S. W. Benson and D. M. Golden, "Advanced Treatise on Physical Chemistry," Vol. 7, H. Eyring, Ed., Academic Press, Chapter 2, in press.

Redox Pattern for Purine and 6-Substituted Purines in Nonaqueous Media. Free Radical Behavior

K. S. V. Santhanam[1] and Philip J. Elving*

Contribution from the Department of Chemistry, University of Michigan, Ann Arbor, Michigan 48104. *Received September 27, 1973*

Abstract: The redox behavior of purine, adenine (6-aminopurine), 6-methylpurine, 6-methoxypurine, 6-methylaminopurine, and 6-dimethylaminopurine has been examined in nonaqueous media (*N*,*N*-dimethylformamide, acetonitrile, and dimethyl sulfoxide) at mercury electrodes by a variety of electrochemical techniques. The purines undergo an initial one-electron (1e) reduction to form the corresponding anionic free radicals, which dimerize (rate constant of 10^3 to 10^5 l. mol^{-1} sec^{-1}). The dimers are oxidized at considerably more positive potential to regenerate the original purines. The rate constant for protonation of the purine anion radical is 1 sec^{-1}. On the addition of weak proton donors, the 1e reduction product is further reduced at the potential of its formation as the result of formation of a more readily reduced protonated species; the reduction attains the level of a 4e process at a mole rate of acid to purine of 3.8–4.0 (total faradaic n for the purines in aqueous media is 4). In the presence of strong acid (perchloric), purine and 6-methylpurine exhibit two 2e waves and the other 6-substituted purines a single 4e wave. The effect of substitution in the 6 position on ease of reducibility is the same in the neutral purines (nonaqueous media) and in positively charged (protonated) purines (aqueous media).

The electrochemistry of biologically important compounds has been the subject of increasing interest in recent years.[2-4] This has been particularly true of purines and pyrimidines related to the constituent bases of the nucleic acids, which direct the synthesis of proteins and are responsible for transfer of genetic infor-

(1) On leave of absence from the Tata Institute of Fundamental Research, Bombay 5, India.

(2) B. Janik and P. J. Elving, *Chem. Rev.*, **68**, 295 (1968); E. Palčeek in "Progress in Nucleic Acid Research and Molecular Biology," Vol. IX, J. N. Davidson and W. E. Cohn, Ed., Academic Press, New York, N. Y., 1969, pp 31–73; A. L. Underwood and R. N. Burnett in "Electroanalytical Chemistry," Vol. 6, A. J. Bard, Ed., Marcel Dekker, New York, N. Y., 1972, pp 1–85; B. Janik and R. G. Sommer, *Biochim. Biophys. Acta*, **269**, 15 (1972); J. W. Webb, B. Janik, and P. J. Elving, *J. Amer. Chem. Soc.*, **95**, 991 (1973); P. J. Elving, J. E. O'Reilly, and C. O. Schmakel in "Methods of Biochemical Analysis," Vol. 21, D. Glick, Ed., Interscience, New York, N. Y., 1973, pp 287–465.

(3) K. S. V. Santhanam and P. J. Elving, *J. Amer. Chem. Soc.*, **95**, 5482 (1973).

(4) P. J. Elving, S. J. Pace, and J. E. O'Reilly, *J. Amer. Chem. Soc.*, **95**, 647 (1973).